 doi:10.20944/preprints202107.0286.v1

Article

Calcium transport along the axial canal in *Acropora*

Yixin Li[1], Xin Liao[2], Chunpeng He[1]* and Zuhong Lu[1]*

[1]State Key Laboratory of Bioelectronics, School of Biological Science and Medical Engineering, Southeast University, Nanjing 210096, China.
[2]Guangxi Academy of Sciences, Guangxi Mangrove Research Center, Guangxi Key Lab of Mangrove Conservation and Utilization, Beihai 536000, China.
* Correspondence: cphe@seu.edu.cn (C.H.); zhlu@seu.edu.cn (Z.L.); tel: 17798550441 (C.H.); 18651800622 (Z.L.)

Abstract: In *Acropora*, the complex canals in a coral colony connect all polyps into a holistic network to collaborate in performing biological processes. There are various types of canals, including calice, axial canals, and other internal canals, with structures that are dynamically altered during different coral growth states due to internal calcium transport. However, few studies have considered the regulation of calcium transport in *Acropora*. In this study, we investigated the morphological changes of the axial canal in six *Acropora muricata* samples by high resolution micro-computed tomography, observing the patterns of the axial canal during the processes of new branch formation and truncated branch rebuilding. We visualized the formation of a new branch from a calice and deposition of the iconic hexactin skeletons in the axial canal. Furthermore, the diameter and volume changes of the axial canal in truncated branches during rebuilding processes were calculated, revealing that the volume ratio of calcareous deposits in the axial canal exhibit significant increases within the first three weeks, returning to levels in the initial state in the following week. This work indicates that the axial canal can transport calcium to form hexactin skeletons in a new branch and rebuild the tip of a truncated branch. The calcium transport along canal network regulates various growth processes, including budding, branching, skeleton forming, and self-rebuilding of an *Acropora* colony. Understanding the changes in canal function under normal and extreme conditions will provide theoretical guidance for restoration and protection of coral reefs.

Keywords: axial canal; reef-building coral; high resolution micro-computed tomography; *Acropora muricata*; calcium transport; deposit

1. Introduction

Coral reefs are highly diverse ecosystems characterized by reef-building corals (1,2). Reef-building corals are essential for maintenance of the biodiversity and ecological functioning of coral reefs (3-6). Among the major reef-building corals, *Acropora* species are responsible for forming the immense calcium carbonate substructure, which is the core of a reef and supports its thin living skin (7). Various types of canals, including calices, axial canals, and other internal canals, support the canal network in an *Acropora* colony and, thus, the physiological processes of coral growth (8,9). The complex canals in a colony connect all polyps into a holistic network to collaborate in performing biological processes (10). Among these processes, the biomineralization carried out in coral polyps deserves attention, as it can sequester carbon and is involved in reef formation (11-15). All polyps in the *Acropora* colony mineralize carbonate or induce calcareous precipitation, and calcium can be carried over considerable distances inside the coral colony toward the zones of maximum growth and calcification (16-19). The canal network in the colony forms a non-radial symmetry transport system for calcium transport during coral growth (20). In this network, the axial canal is unique, being the largest canal along the branch center in an *Acropora* colony, and its extension reveals the growth directions of the coral branch (8,9). However, the role of the axial canal in an *Acropora* colony and details of its structural

 doi:10.20944/preprints202107.0286.v1

transformation during coral growth remain obscure, as literature on this subject is scarce (21). Meanwhile, although the transport of organic compounds within coral colonies has been suggested in various works, most are inferences based on markers or elemental measurements (22-26), rather than direct visualizations of structural changes in coral colonies.

The non-transparent skeleton influences direct observation of the distribution, parameters, and relationships among canals in coral colonies (20). Experiments with traditional biological methods have provided very limited and circumstantial evidence about how the axial canal participates in coral growth and calcium transport (27-29). To solve this problem, high-resolution computed tomography (HRCT) has gained increasing attention (30,31). HRCT can be used to non-destructively capture the morphology and internal structure of coral colonies (32,33). Compared with traditional biological techniques, like scanning electron microscope (SEM) and grinding sections, HRCT has multiple advantages (10). Skeletal reconstruction through HRCT can be used directly on living corals, for which complicated and potentially destructive preparations, such as pickling or fixing, are not required (34). HRCT can reveal the delicate internal skeletal structures in coral colonies that are easily destroyed using traditional techniques (35). Moreover, all colony skeletal information can be captured in detail at once (36). Any position and section in a colony can be observed as needed, saving coral resources and eliminating the burden of multiple measurements with complete sample analysis achieved in a single process (37).

In this study, we explored calcium transport in the axial canal during different physiological states of coral growth by comparing the skeleton and canal morphology between two extreme growing states. One is the growth process of a new branch in a coral colony, and the other is the self-rebuilding process of truncated branches. We used HRCT to reconstruct six representative samples of *Acropora muricata*, which is common and frequently a dominant species in coral reefs. Furthermore, we calculated related parameters of the axial canal during new branch formation and truncated branch rebuilding. The pattern regulation of axial canals in colony formation was visualized in both of these growth states, revealing the regulatory processes of the axial canal in the calcium transport system. Thus, calcium transport along the axial canal in *Acropora* could be determined.

This study expands our understanding of calcium transport patterns in *Acropora*, which is conducive to the breeding and protection of reef-building corals (38-41). In addition, studying the internal structure and function of coral canals provides theoretical guidance for the current research into constructing artificial reefs (42,43) and reconstructing coral reefs through 3D printing (44-47), laying a scientific foundation for the establishment of an improved coral reef restoration system (41, 48-50).

2. Results

2.1. The morphology and internal structure of axial canals in A. muricata

The three-dimensional skeletal structures of six *A. muricata* samples were reconstructed by HRCT, including both the surface morphology and the internal structural characteristics, allowing us to study the structural pattern of the skeletons around the axial canal in the processes of coral branch formation (Fig. 1, Fig. 2).

The structures of the skeletons in the apical region of the coral branch are porous. Complex skeletons form a net-like external surface around the axial canal, while skeletal protrusions with the characteristic of hexactin can be found in the cavity of the axial canal (Fig. 1A). In stark contrast, the skeletons around the cavity of the calice, the area in which a coral polyp lives, are relatively smooth and nearly nonporous (Fig. 1B). We also observed that the transformation in the skeleton and cavity structure at the tip of a newly formed branchlet occurred in three steps (Fig. 1C–E), which is evidence of the high activity occurring during coral growth. From step 1 to step 3, the morphological characteristics gradually change from calice-like to axial canal-like with advancement of the growth process. During the transformation from a calice to the axial canal, the skeletons around the canal become thicker, and complex internal canals are formed in the skeleton (Fig. 1–E).

Preprints (www.preprints.org) | NOT PEER-REVIEWED | Posted: 13 July 2021 doi:10.20944/preprints202107.0286.v1

The hexactin skeletons, which are the signals in the axial canal of *A. muricata*, are gradually formed from the calice to step 2 (Fig. 1B–D). Until step 2, the structures of both the hexactin skeletons and axial canal in the new branch are similar to those of the old branch (Fig. 1B,D), and the only difference in the axial canal between step 2 and step 3 is the length of the cavity (Fig. 1D,E).

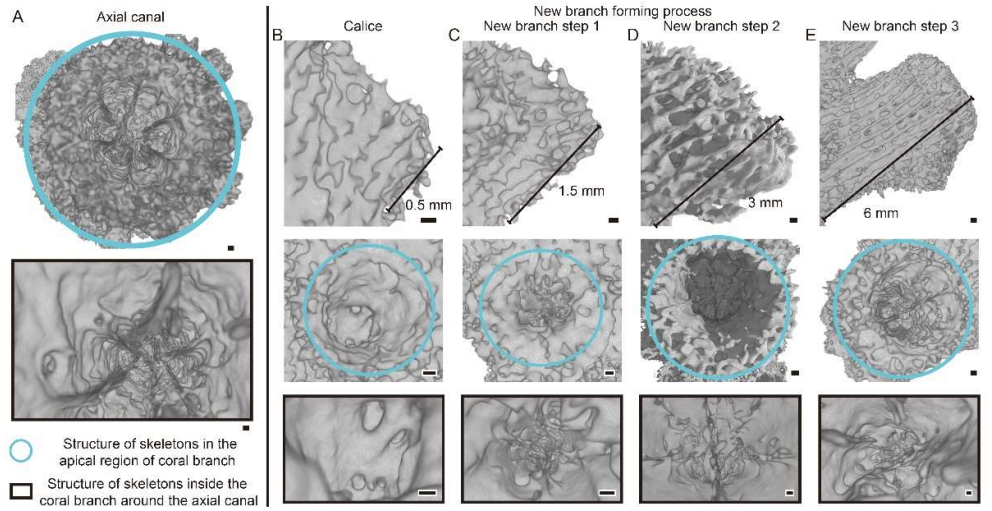

Figure 1. Structure of the skeleton surrounding the axial canal during the processes of new branch formation in *A. muricata*. (**A**) The axial canal in a healthy and mature coral branch. (**B-E**) A calice transfers into an axial canal of the new branch. Scale: 0.1 mm.

During the tip rebuilding process in truncated branches, which are involved in regulation of another extreme growth event in the coral colony, an unusual phenomenon appears in the cavity of the axial canal (Fig. 2A–D). The structure of a truncated branch is similar to a normal branch at day 0, and the only calcareous deposits in the axial canal are iconic hexactin skeletons (Fig. 1A, Fig. 2A). When the new tip is rebuilt at the truncated area around day 14, irregularly shaped calcareous deposits appear in the cavity of the axial canal (Fig. 2B). Until day 21, the axial canal in the rebuilt tip is nearly filled with calcareous deposits, and various calcareous deposits even appear in the cavity below the truncated area (Fig. 2C). However, all those sediments disappear after the rebuilding process at day 28 (Fig. 2D), and the branch shape returns to the status shown in Fig. 1A.

Preprints (www.preprints.org) | NOT PEER-REVIEWED | Posted: 13 July 2021 doi:10.20944/preprints202107.0286.v1

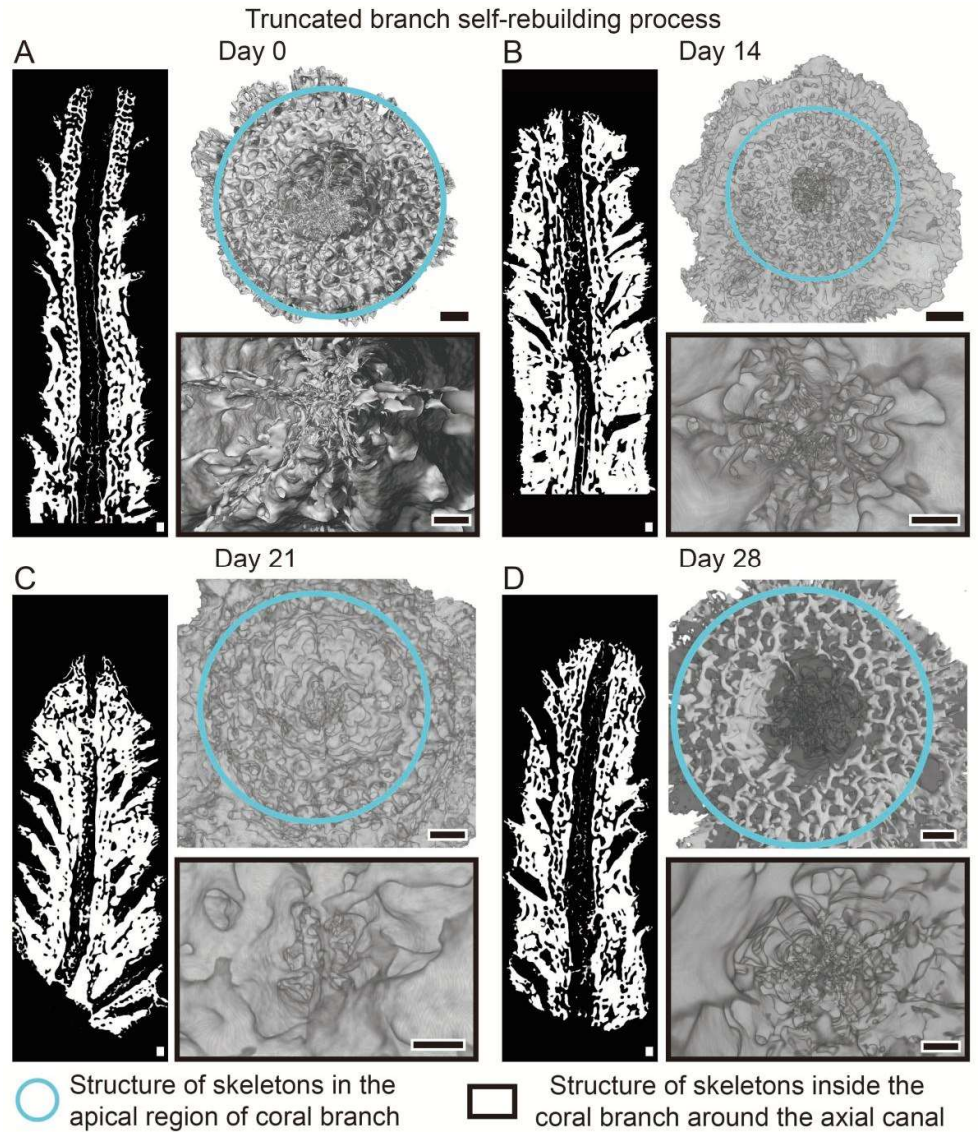

Figure 2. Structure of the skeleton surrounding the axial canal during the process of truncated branch self-rebuilding in *A. muricata*. (**A–D**). The rebuilding process of the truncated branch. Scale: 0.5mm.

2.2. The morphological changes of the axial canal reveal regulation of calcium transport

In *A. muricata*, the polyp network is complex because multiple canal types are involved. A large number of internal canals connect the axial canals and all polyp calices into a holistic network to collaborate in performing biological processes within a single coral colony. To illustrate the role of the axial canal in calcium transport, we created 3D reconstructions of the axial canals and calices hidden in coral skeletons to obtain information related to calcium transport during the processes of new branch formation and truncated branch rebuilding (Fig. 3–5).

Preprints (www.preprints.org) | NOT PEER-REVIEWED | Posted: 13 July 2021 doi:10.20944/preprints202107.0286.v1

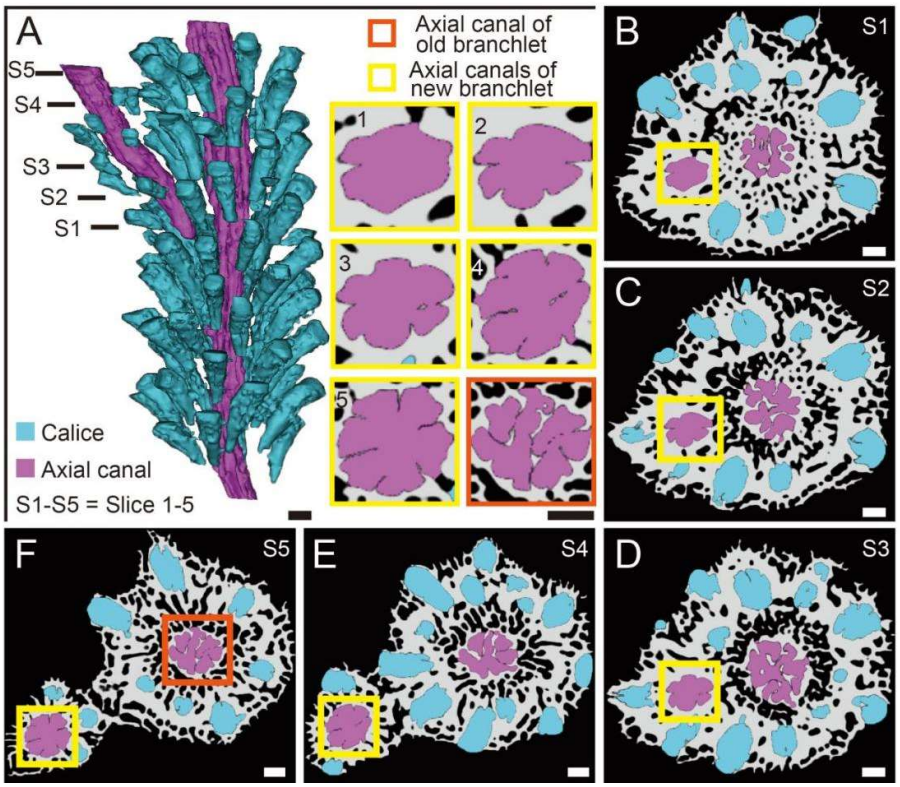

Figure 3. 3D canal reconstruction visualizing the axial canal formation during branch-born processes in *A. muricata*. (**A**) An *A. muricata* branch with a newborn branchlet. (**B**,**C**,**D**,**F**) The S1–S5 cross-sections reveal the calice–axial canal transformation during the birth of a new branchlet. Scale bars: 1 mm.

In the *A. muricata* branch, the distance among adjacent calices is similar, and the calices circle the axial canal along the growth direction. The distances from each calice bottom to the axial canal are also similar, and complex internal canals link them together (Fig. 3). When an *A. muricata* colony branches, the axial canal reveals the branch growth direction, and the new axial canal appears in the center of the newborn branchlet (Fig. 3A). The newborn axial canal first appeared at the stage shown in slice 1 (Fig. 3B). At that time, its cross-section was approximately circular, like that of a common calice. The distance between the bottom of the new axial canal and that of the old axial canal was approximately 1.5 mm, and the distance to adjacent calices was approximately 2 to 3 mm (Fig. 3B). The shape, location, and distribution of the axial canals were similar to those of the calices at this stage. In slice 2, the cross-section of the new axial canal started to present a hexactinal shape, like that of an old axial canal, and two new calices emerged close to this younger one (Fig. 3C). At the stage of slice 3, the cross-section of the new axial canal further approached a hexactinal shape (Fig. 3D), and a piece of skeleton appeared inside its axial canal. Additionally, the skeleton outline of the new branchlet tended to be patterned. In slice 4, new calices appeared between the new and old axial canals, while the connection between the newborn branchlet and the old branch consisted of only a piece of skeleton and an internal canal (Fig. 3E). Up to slice 5, the new axial canal was surrounded by more calices, and its cross-sectional shape was the same as that of the old one (Fig. 3F). The new branchlet separated from the old one, and axial canal formation was complete. This pseudotime process from slices 1 to 5 shows the transformation of a newborn axial canal from a calice type to a mature state and the birth pattern of a new branchlet. The metamorphosis from calice to axial canal indicates why leading polyps are distributed in *A.*

Preprints (www.preprints.org) | NOT PEER-REVIEWED | Posted: 13 July 2021 doi:10.20944/preprints202107.0286.v1

muricata branch tips and suggests the budding process in a new branchlet (Fig. 6). Meanwhile, the slices of the axial canal in Figure 3A also reveal the formation of hexactin skeletons in the axial canal during the stages from calice to step 2 in Figure 1.

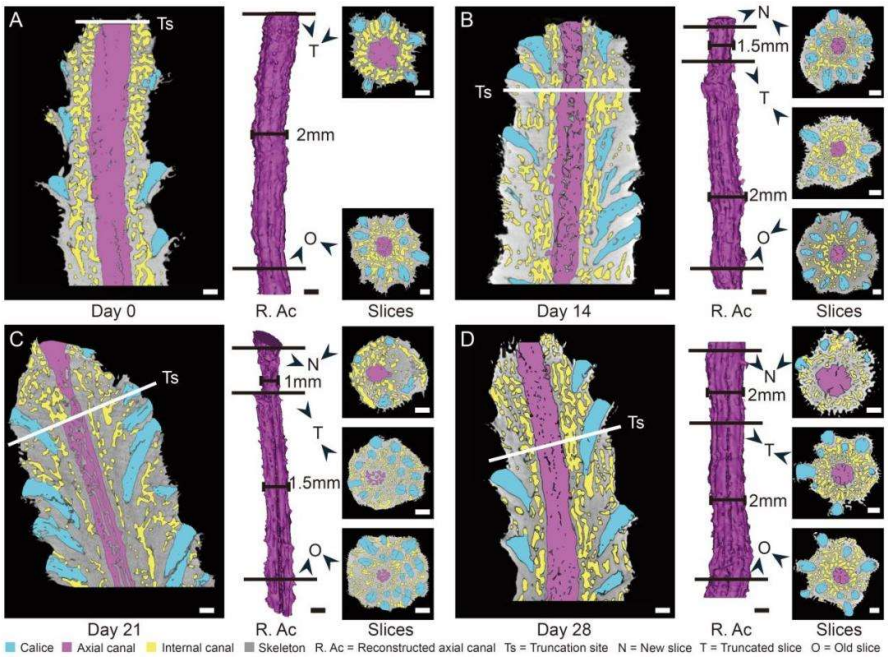

Figure 4. 3D canal reconstructions revealing calcium transport along the axial canal under the truncated branch rebuilding process in *A. muricata*. (**A**) In 0-day samples, the columnar axial canal has few skeletal structures scattered inside it, and its cross-sectional diameter is about 2.0 mm. (**B**) In 14-day samples, the number of inner skeletal structures within the axial canal is increased. The cross-section diameter of the newborn part of the axial canal is about 1.5 mm, thinner than the older part. (**C**) In 21-day samples, the inner skeletons increase and occupy nearly half of the axial canal space. The cross-section diameter of the axial canal is about 1.0 mm in the newborn part, and 1.5 mm in the older part. (**D**) In 28-day samples, there are fewer inner skeletons left in the axial canal, and the cross-sectional diameter of the axial canal is similar to the day-0 group. Scale bars: 1 mm.

We also investigated the rebuilding process of a branch and its axial canal in *A. muricata* through a truncation experiment and a 3D canal reconstruction (Fig. 4). The columnar axial canal in the day 0 group had a smooth surface with few skeletal structures (hexactin skeletons) scattered inside it, and its cross-sectional diameter was approximately 2.0 mm (Fig. 4A). Obvious changes appeared in the structure of the axial canal beginning at day 14, with the appearance of new calcareous deposits in the axial canal, except for where there are hexactin skeletons (Fig. 4B). The number of inner skeletons within the axial canal increased, and the surface of the axial canal became rough with more concave structures, indicating that the skeleton around the axial canal was proliferating inward. The cross-sectional diameter of the newborn part of the axial canal was approximately 1.5 mm thinner than its previous diameter (Fig. 4B). By day 21, the coral branch entered the peak period of the rebuilding process, and its axial–canal structure had changed the most (Fig. 4C). The calcareous deposits had been connected into many long column-like structures and penetrated the axial canal deeply, occupying nearly half of the axial canal space. The cross-sectional diameter was approximately 1.0 mm, half of the diameter of the day 0 group. Amazingly, the cross-sectional diameter of the previous axial canal reduced to 1.5 mm, suggesting that a long-distance calcium transport was also involved in this rebuilding process (8). In the 28-day samples, only the hexactin skeletons were left in the axial canals, and the cross-sectional diameter of the axial canal was similar to that of the day 0 group (Fig. 4D). The surface of the axial canal was smooth again, indicating that the rebuilding process of the branch was almost complete. This rebuilding process, shown in

Preprints (www.preprints.org) | NOT PEER-REVIEWED | Posted: 13 July 2021 doi:10.20944/preprints202107.0286.v1

Fig. 4, was a kind of extreme growth pattern. These related 3D reconstructions suggest that the axial canal plays an important role in the truncated branch rebuilding process in *A. muricata*, implying that the axial canal is responsible for calcium transport during the self-healing process. Meanwhile, this phenomenon indicates that the canals in one *A. muricata* branch, represented by the axial canal, can connect the polyps in the branch into a network to regulate the rebuilding process of coral growth.

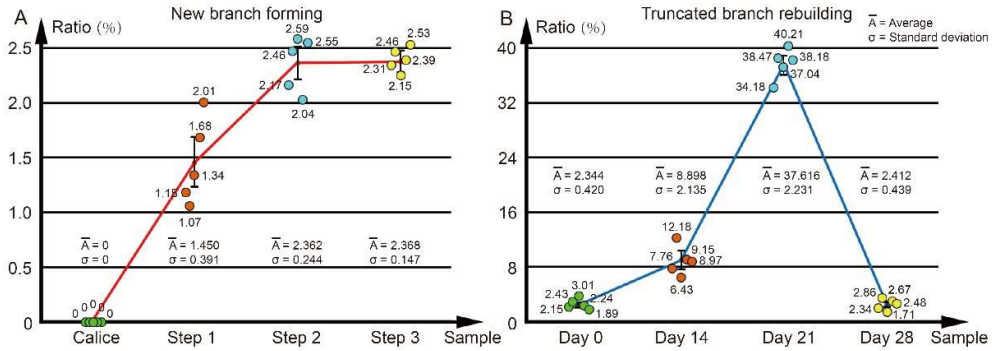

Figure 5. Volume ratio of calcareous deposits in the axial canal under different growth processes. (**A**) The volume ratio changes during the new branch formation process. (**B**) The volume ratio changes during the truncated branch rebuilding process.

To quantify the calcareous deposits in the axial canal during the two growth processes, we calculated the value of each sample in this study (Fig. 5, Method 4.6). No calcareous deposits are found in the calice before its transformation to the axial canal in the new branch (Fig. 5A). During the new branch formation process, calcium can be carried along the new axial canal to form its hexactin skeleton, which is shown as an increase in the volume ratio of calcareous deposits (from 0% to 2.362%) between the states of the calice and step 2 (Fig. 5A). The truncated branch rebuilding process leads to a huge increase (from 2.344% to 37.616%) in the volume ratio of calcareous deposits from day 0 to day 21, and the ratio returns to the initial state after the self-rebuilding (Fig. 5B).

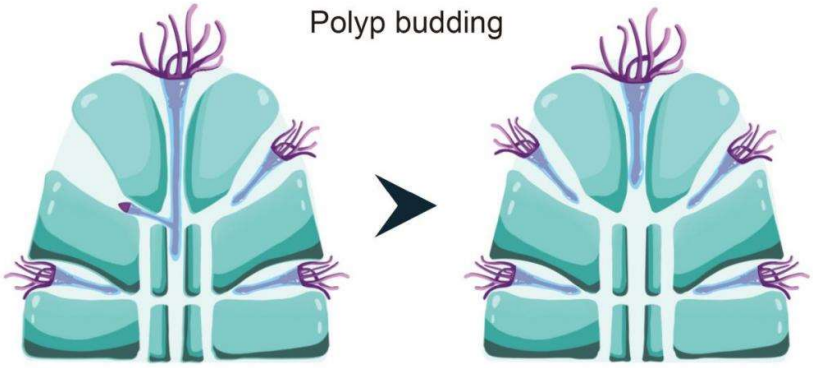

Figure 6. Polyp budding schematic according to the canal network reconstructions. The polyp buds after the mineralization of new skeletons and canals, and the newly budded polyp migrates to its new calice through the complex internal canal, which connects the axial canal and calices.

3. Discussion

3.1. The canal network regulates the budding and branching process

 doi:10.20944/preprints202107.0286.v1

In this study, we reconstructed the axial canal and the skeletons around its cavity through HRCT to investigate the role of the canal network in the budding, branching, calcium transport, and self-healing processes of coral growth (Fig. 1–5).

The canal network, which makes up an apparent polyp network, is the basic foundation of coral growth (10,51). As the largest canal in the network of an *A. muricata* colony, the axial canal is transformed from specific calices (Fig. 1B–E, Fig. 3). The chosen calice transforms into the axial canal of new branch following the regulation of the canal network in the branching process (Fig. 3). Meanwhile, canal network reconstructions reveal that in the newly formed branchlet, new calices distributed near their axial canal may only obtain polyps from the new axial canal (Fig. 3A,E,F), which also suggests the budding patterns in the new branchlet (Fig. 6). Although how a coral colony selects a specific calice and induces its transition into a new axial canal during coral branching is still unclear, the visualization of this process provides a basis for studies in this area.

3.2. Calcium transport along the axial canal under different coral growth states

Calcium can be carried through the canal network toward the growth area of the coral colony (19). According to previous studies of the transport system in *Acropora* branches, the axial canal is not involved in the transport of hydroplasm (20). However, this study revealed that the axial canal plays an important role in calcium transport during two extreme growth states: truncated branch self-rebuilding, and new branch formation (Fig. 3, Fig. 4). The analysis and speculation regarding calcium transport along the axial canal were mainly based on the visualization and parameter calculations of the calcareous deposits in the canal cavity (Fig. 3–5).

In truncated branches, the most active area of calcification is the rebuilding tip at the truncated region and, thus, calcium is delivered to the rebuilding area through the transport system in a colony. Although the axial canal does not play a major role in the transport of hydroplasm in *Acropora*, extreme growing process, like truncated branch rebuilding, may change the role of the axial canal in the transport system of *A. muricata* (Fig. 2, Fig. 4). A large amount of calcium is transported through the axial canal to the truncated region to rebuild a coral branch, and the increase of calcium content in the axial canal also leads to a reduction in the deposited calcareous skeleton, leading to a decrease in the diameter of the axial canal cavity (Fig. 4B,C). During the peak period of the branch rebuilding process, in the axial canal, the diameter at the truncated area is reduced by half and the diameter at areas prior to this is reduced by a quarter, while nearly forty percent of the cavity is filled by calcareous deposits (Fig. 4C, Fig. 5B). After the self-healing of a coral colony, this calcium transportation stops, and the depositing of calcareous skeletons is recast due to the decreased calcium content in the axial canal. At this stage, the structure of the cavity returns to its initial form (Fig. 4D).

The formation of a new branchlet during coral branching will also lead to calcium transport in the colony. In this extreme growing process, calcium transport takes place in the axial canal during the formation of hexactin skeletons in the axial canal (Fig. 1B–D, Fig. 3, Fig. 5A). However, this phenomenon does not appear after step 2, which means that with the end of the hexactin skeleton formation, the formation of a new branch begins to approach the regular coral growth state, and the calcium transport in the axial canal also tends to stop (Fig. 1E, Fig. 5A). This indicates that the calcium transportation through the axial canal may only happen during the self-healing and branching processes in the coral colony, suggesting further study is required. This truncated branch rebuilding experiment on *A. muricata* also suggests that the polyp network of the canal system makes coral branch growth a kind of integral behavior.

4. Methods and Materials

4.1. Sample collection

Preprints (www.preprints.org) | NOT PEER-REVIEWED | Posted: 13 July 2021 doi:10.20944/preprints202107.0286.v1

All six *A. muricata* samples in this study were collected from the Xisha Islands (Paracel Islands, 16°53′N, 112°17′E) of the South China Sea, in 2018. All samples, which occurred in large arborescent colonies forming thickets, were found in tropical shallow reefs of marine neritic, from depths of about 5–10 m. The daily mean temperature was between 23.2 and 29.2 °C. The coral samples were kept whole and housed in our laboratory coral tank, where all conditions were simulated to reflect those of their habitat in the South China Sea. These samples were kept in the tank for about one to three months before the HRCT test. Among these *A. muricata* samples, one was a colony (about 20 cm × 20 cm × 25 cm), and the other five were coral branches (length of about 4 cm, diameter between 0.5 and 1 cm) from different colonies.

4.2. Coral culture system

Our coral samples were cultured with the laboratory auto calibration balance system (52) in a standard RedSea® tank (redsea575, Red Sea Aquatics Ltd), following the Berlin Method. The temperature was kept at 25 °C, and the salinity (Red Sea Aquatics Ltd) was 1.025. The culture system was maintained using a Protein Skimmer (regal250s, Reef Octopus), a water chiller (tk1000, TECO Ltd), three coral lamps (AI®, Red Sea Aquatics Ltd), two wave devices (VorTech™ MP40, EcoTech Marine Ltd), and a calcium reactor (Calreact 200, Reef Octopus).

Around 20 kg of live rocks, which were also collected from the South China Sea, were placed in the coral tank. These live rocks provided the structure of the growth environment and some necessary microorganisms. We also weekly added minerals to the tank, including Mg, Ca, KH, K, I, and Fe.

4.3. HRCT test

We analyzed six *A. muricata* samples from the South China Sea using three dimensional models constructed with the 230 kV latest-generation X-ray microfocus computed tomography system (Phoenix v|tome|x m, General Electric (GE)), at Yinghua NDT, Shanghai, China. Two-dimensional image reconstructions of each specimen from matrices of scan slices were assembled using proprietary software from GE. The relevant parameters are shown in Table 1.

Table 1. Parameters of the HRCT tests.

Sample	Voltage	Current	Voxel size	Timing	Number of images	Image width	Image height
Acropora colony one	150 kV	180 μA	37 μm	1 s	2000	3990 pixels	4000 pixels
Acropora branch one	130 kV	60 μA	6 μm	500 ms	1500	2800 pixels	4000 pixels
Acropora branch two	120 kV	115 μA	12 μm	500 ms	2400	1980 pixels	2000 pixels
Acropora branch three	130 kV	60 μA	6 μm	500 ms	1500	2800 pixels	4000 pixels
Acropora branch four	130 kV	100 μA	9 μm	500 ms	2500	1985 pixels	2000 pixels
Acropora branch five	160 kV	70 μA	9 μm	500 ms	1600	1500 pixels	4000 pixels

.4.4. Internal canal reconstruction

Slice data derived from the scans were then analyzed and manipulated using VG software. The 3D reconstructions were created in Mimics (v20.0) software and VG Studio

Max (v3.3.0), following the method as previously described (10). The images of the reconstructions were exported from Mimics and VG Studio Max and finalized in Adobe Photoshop CC 2019 and Adobe Illustrator CC 2019.

4.5. Truncation experiment

We selected four groups of *A. muricata* branches of a similar size (4 cm) and shape (a column with a diameter between 5 mm and 1 cm from the tip to the bottom) to truncate their tips at same position and culture them in the same environments. The truncated samples were assessed using HRCT at day 0, 14, 21, and 28 (*A. muricata* branch 2–5) for HRCT detection.

4.6. Calculation of the calcareous deposit volume ratio in the axial canal

The calculation of the calcareous deposit volume ratio in the axial canal was performed in the VG Studio Max 3.3. First, we used "surface determination" to distinguish the area of skeleton reconstruction and porosity. Then, we calculated the volume of calcareous deposits, and used the "erode/dilate" mode to select the entire area of the axial canal. After that, we used the "porosity/inclusion analysis module" to reconstruct the internal porosity for the volume calculation. Thus, with the volume of both calcareous deposits and the axial canal, we were able to obtain the calcareous deposit volume ratio in the axial canal of each sample.

Data Availability Statement: The HRCT data that support the findings of this study are available to share. You may download the HRCT reconstruction data through the following links. *Acropora muricata* colony: doi:10.5061/dryad.wdbrv15nm (https://datadryad.org/stash/share/rWeA0hUxlu__l8sUEdkAIPAtTq3UGbxsYw095ktjWhs), *Acropora muricata* branch 1: doi:10.5061/dryad.ghx3ffbnh (https://datadryad.org/stash/share/7YfZPthkA9VP6Djw0OPRyKGhXAP6L-Bb5XYMYVA4ZVQ), *Acropora muricata* branch 2: doi:10.5061/dryad.p2ngf1vq4 (https://datadryad.org/stash/share/V3iXkB8Fk2M9nvELjGCyOJsRzpNFyBBrKo34oGdwu7M), *Acropora muricata* branch 3: doi:10.5061/dryad.08kprr524 (https://datadryad.org/stash/share/8SPvv12ifZv_wEf2Uy61PauSkL0oX8tF1iR9lf74DIM), *Acropora muricata* branch 4: doi:10.5061/dryad.8w9ghx3mb (https://datadryad.org/stash/share/ZTV11TYSlf5Kgqnfo1UZBdS8KabYJSPrrL7U6jg6Jv0), *Acropora muricata* branch 5: doi:10.5061/dryad.pnvx0k6m8 (https://datadryad.org/stash/share/e94f4E80T8ZLfC-YXOACLdMoPMcl4AfVLwt6xdLvNb8)

Author Contributions: Y. L., C. H. and Z. L. conceived the project. Y. L. wrote the paper and produced the figures. Y. L. reconstructed the images and performed the biological analyses. X. L. collected the coral samples. Y. L., C. H. and Z. L. edited the paper. All authors discussed and commented on the data.

Acknowledgments: This study was supported by the Open Research Fund Program of Guangxi Key Lab, of Mangrove Conservation and Utilization (Grant No. GKLMC-202002).

Declaration of Interests: The authors declare no competing interests.

References

1. Bostrom-Einarsson, L., et al. Coral restoration - A systematic review of current methods, successes, failures and future directions. *PLOS One*. **15** (1), e0226631 (2020).
2. Costanza, R., et al. Changes in the global value of ecosystem services. *Glob. Environ. Chang.* **26**: 152-158 (2014).
3. Malik, A., et al. Molecular and skeletal fingerprints of scleractinian coral biomineralization: From the sea surface to mesophotic depths. *Acta Biomaterialia*. **120**, 263-276 (2021).
4. Gratwicke, B., Speight, M. R. The relationship between fish species richness, abundance and habitat complexity in a range of shallow tropical marine habitats. *Journal of Fish Biology*. 66 (**3**): 650-667 (2005).
5. Fontaneto, D., Sanciangco, J. C., Carpenter, K. E., Etnoyer, P. J., Moretzsohn, F. Habitat Availability and Heterogeneity and the Indo-Pacific Warm Pool as Predictors of Marine Species Richness in the Tropical Indo-Pacific. *PLoS one*. **8** (2): e56245 (2013).
6. Hatcher, B. G., Johannes, R. E., Robertson, A. J. Conservation of Shallow-water Marine Ecosystems. *Oceanography and Marine Biology: An Annual Review*. **27**: 320 (1989).

7. Wallace, C. C., Rosen, B. R. Diverse staghorn corals (*Acropora*) in high-latitude Eocene assemblages: implications for the evolution of modern diversity patterns of reef corals. *Proceedings of the Royal Society B: Biological Sciences*. **273** (1589), 975-982 (2006).
8. Wells, J. W. The nomenclature and type species of some genera of recent and fossil corals. *American Journal of Science*. **31** (182), 97-134 (1936).
9. Madin, J. S., et al. The Coral Trait Database, a curated database of trait information for coral species from the global oceans. *Scientific Data*. **3**: 160017 (2016).
10. Li, Y. et al. The 3D reconstruction of *Pocillopora* colony sheds light on the growth pattern of this reef-building coral. *iScience*. **23**, 101069 (2020).
11. Moura, R. L., et al. An extensive reef system at the Amazon River mouth. *Science Advances*. **2**(4): e1501252 (2016).
12. Pablo, J. Life and Death of Coral Reefs. *Fisheries Research*. **48**(3): 53-74 (2004).
13. Alongi, D. M. Carbon Cycling and Storage in Mangrove Forests. *Annual Review of Marine Science, Vol 6*. **6**: 195-219 (2014).
14. Tambutte, S., Holcomb, M., Ferrier-Pages, C., Reynaud, S., Tambutte, E., Zoccola, D., Allemand, D. Coral biomineralization: From the gene to the environment. *Journal of Experimental Marine Biology and Ecology*. **408**(1-2): 58-78 (2011).
15. Conci, N., Vargas, S., Worheide, G. The Biology and Evolution of Calcite and Aragonite Mineralization in Octocorallia. *Frontiers in Ecology and Evolution*. **9**: 623774 (2021).
16. Levy, S., et al. A stony coral cell atlas illuminates the molecular and cellular basis of coral symbiosis, calcification, and immunity. *Cell*. **184**(11), 2973 (2021).
17. Dzakula, B. N., Fermani, S., Dubinsky, Z., Goffredo, S., Falini, G., Kralj, D. In Vitro Coral Biomineralization under Relevant Aragonite Supersaturation Conditions. *Chemistry-A European Journal*. **25**(45), 10616-10624 (2019).
18. Sugiura, M., Yasumoto, K., Iijima, M., Oaki, Y., Imai, H. Morphological study of fibrous aragonite in the skeletal framework of a stony coral. *Crystengcomm*. **23**(20): 3693-3700 (2021).
19. Taylor D.L. Intra-colonial transport of organic compounds and calcium in some Atlantic reef corals. *Proceedings, Third International Coral Reef Symposium*. **1**. 431–436 (1977).
20. Marfenin, N. N. Non-radial symmetry of the transport system of *Acropora* corals. *Invertebrate Zoology*. **12** (1), 53-59 (2015).
21. Gladfelter E.H. Circulation of fluids in the gastrovascular system of the reef coral *Acropora cervicornis*. *Biological Bulletin*. **165**. 619-638 (1983).
22. Marfenin, N. N. Colony morphology and transport system in two species of hermatypic coral genus Acropora. *Zoologichesky Zhurnal*. **62**(5): 131983 (1983).
23. Taylor D. L. Intra-colonial transport of organic compounds and calcium in some Atlantic reef corals. *Proceedings, Third International Coral Reef Symposium*. **1**, 431–436 (1977).
24. Parrin, A. P., Netherton, S. E., Bross, L. S., McFadden, C. S., Blackstone, N. W. Circulation of fluids in the gastrovascular system of a stoloniferan octocoral. *Biological Bulletin*. **219**, 112–121 (2010).
25. DeCarlo, T. M., Ross, C. L., McCulloch, M. T. Diurnal cycles of coral calcifying fluid aragonite saturation state. *Marine Biology*. **166**(3): 28 (2019).
26. Knebel, O., et al. Porites Calcifying Fluid pH on Seasonal to Diurnal Scales. *Journal of Geophysical Research-Oceans*. **126**(3): e2020JC016889 (2021).
27. Bonesso, J. L., Leggat, W., Ainsworth, T. D. Exposure to elevated sea-surface temperatures below the bleaching threshold impairs coral recovery and regeneration following injury. *PeerJ*. **5**: e3719 (2017).
28. Chindapol, N., Kaandorp, J. A., Cronemberger, C., Mass, T., Genin, A. Modelling growth and form of the scleractinian coral *Pocillopora verrucosa* and the influence of hydrodynamics. *PLoS Comput. Biol.* **9**: e1002849 (2013).
29. Welsh, R. M., Rosales, S. M., Zaneveld, J. R., Payet, J. P., McMinds, R., Hubbs, S. L., Thurber, R. L. V. Alien vs. predator: bacterial challenge alters coral microbiomes unless controlled by Halobacteriovorax predators. *PeerJ*. **5**: e3315 (2017).
30. Knackstedt, M. A., Arns, C. H., Senden, T. J., Gross, K. Structure and properties of clinical coralline implants measured via 3D imaging and analysis. *Biomaterials*. **27**: 2776-2786 (2006).
31. Kruszynski, K., Liere, R. V., Kaandorp, J. A. An Interactive Visualization System for Quantifying Coral Structures. *The Eurographics Association*. (2006).
32. Beuck, L., Vertino, A., Stepina, E., Karolczak, M., Pfannkuche, O. Skeletal response of Lophelia pertusa (Scleractinia) to bioeroding sponge infestation visualised with micro-computed tomography. *Facies*. **53**: 157-176 (2007).
33. Kruszynski, K., Kaandorp, J. A., Liere, R. V. A computational method for quantifying morphological variation in scleractinian corals. *Coral Reefs*. **26**: 831-840 (2007).
34. Nishikawa, T., et al. Physical characteristics and interior structure of coral skeleton as a bone scaffold material. *J. Oral. Tissue Eng*. **7**: 121-127 (2009).
35. Janiszewska, K., Stolarski, J., Benzerara, K., Meibom, A., Mazur, M., Kitahara, M. V., Cairns, S. D. A unique skeletal microstructure of the deep-sea micrabaciid scleractinian corals. *J. Morphol*. **2**: 191-203 (2011).
36. Janiszewska, K., Jaroszewicz, J., Stolarski, J. Skeletal ontogeny in basal scleractinian micrabaciid corals. *J. Morphol*. **3**: 243-257 (2013).
37. Tambutté, E., et al. Morphological plasticity of the coral skeleton under CO2-driven seawater acidification. *Nat. Commun*. **6**: 7368 (2015).
38. Lirman, D., Schopmeyer, S., Galvan, V., Drury, C., Baker, A. C., Baums, I. B. Growth dynamics of the threatened caribbean staghorn coral Acropora cervicornis: Influence of host genotype, symbiont identity, colony size, and environmental setting. *PloS one*. **9**(9): e107253 (2014).

39. Young, C. N., Schopmeyer, S. A., Lirman, D. In situ coral nurseries serve as genetic repositories for coral reef restoration after an extreme cold-water event. *Restoration Ecology*. **20**(6), 696-703 (2012).
40. Lirman, D., Schopmeyer, S. Ecological solutions to reef degradation: optimizing coral reef restoration in the Caribbean and Western Atlantic. *PeerJ*. **4**: e2597 (2016).
41. Horoszowski-Fridman, Y. B., Izhaki, I., Rinkevich, B. A review of reef restoration and coral propagation using the threatened genus *Acropora* in the Caribbean and western Atlantic. *Bulletin of Marine Science*. **88** (4): 1075-1098 (2012).
42. Matus, I. V., Alves, J. L., Gois, J., da Rocha, A. B., Neto, R., Mota, C. D. Effect of 3D printer enabled surface morphology and composition on coral growth in artificial reefs. *Rapid Prototyping Journal*. **27**(4), 692-706 (2021).
43. Wolfe, K., Mumby, P. J. Rubble Biodiversity Samplers: 3D-printed coral models to standardize biodiversity censuses. *Methods in Ecology and Evolution*. **11**(11): 1395-1400 (2020).
44. Wangpraseurt, D., et al. Bionic 3D printed corals. *Nature Communications*. **11**(1): 1748 (2020).
45. Ruhl, E. J., Dixson, D. L. 3D printed objects do not impact the behavior of a coral-associated damselfish or survival of a settling stony coral. *PLoS one*. **14**(8): e0221157 (2019).
46. Sun, C. Y., Marcus, M. A., Frazier, M. J., Giuffre, A. J., Mass, T., Gilbert, P. U. P. A. Spherulitic Growth of Coral Skeletons and Synthetic Aragonite: Nature's Three-Dimensional Printing. *ACS Nano*. **11**(7), 6612-6622 (2017).
47. Young, G. C., Dey, S., Rogers, A. D., Exton, D. Cost and time-effective method for multiscale measures of rugosity, fractal dimension, and vector dispersion from coral reef 3D models. *PLoS one*. **12**(4): e0175341 (2017).
48. Yanovski, R., Abelson, A. Structural complexity enhancement as a potential coral-reef restoration tool. *Ecological Engineering*. **132**: 87-93 (2019).
49. Page, C. A., Muller, E. M., Vaughan, D. E. Microfragmenting for the successful restoration of slow growing massive corals. *Ecological Engineering*. **123**: 86-94 (2018).
50. Bostrom-Einarsson, L., et al. Coral restoration - A systematic review of current methods, successes, failures and future directions. *PLoS one*. **15**(1), e0226631 (2020).
51. Liu, J., Wang J., Guo, D., Shi, G. Three-Dimensional Morphology and Stratigraphic Structure of Coral Reef in Xisha and Nasha Islands. *Advances in Geosciences*. **9** (2), 61-68 (2019).
52. Li, Y. et al. Coral growth monitoring in 24 weeks with laboratory auto calibration balance system. *Journal of Coastal Research*. **108**, 288-293 (2020).